due to changes of the ligands surrounding the $M_3X_4$ core. For example, the LUMO (also $14a_1$) and the MOs higher in the $Mo_3S_4$ case correlate well with the virtual MOs in Figure 4, but the HOMO now is the $13a_1$ orbital, which is mainly Mo-P bonding.

A significant difference in the electronic structures of the six-electron compounds with different $\mu$-X atoms can be seen immediately from Figure 4. Compared to case in the compound with the $\mu$-Cl atoms, very large HOMO-LUMO energy gaps, 1.53 and 1.22 eV, have been predicted for the two six-electron compounds with $\mu$-O and $\mu$-S atoms, respectively. The large HOMO-LUMO gap is apparently caused by the very strong interaction between the metal atoms and the $\mu$-O or $\mu$-S atoms, which raises the energy of the LUMOs in the compounds due to their Mo-($\mu$-X) antibonding character. As shown by our calculations, the $14a_1$ orbitals (the LUMOs) in $[Mo_3O_4(OH)_6(H_2O)_3]^{2-}$ and $[Mo_3S_4Cl_6(PH_3)_3]^{2-}$ have considerably larger contributions from the $\mu$-O atms (27%) and the $\mu$-S atoms (34%), respectively, than those provided by the $\mu$-Cl atoms (12%) to the corresponding orbital in $[Mo_3OCl_3(OH)_6(H_2O)_3]^{+}$. The contour plots of the orbitals (Figure 3c,d) further indicate that the character of the $14a_1$ orbitals is dominated by the Mo-($\mu$-X) (X = O, S) antibonding rather than the M-M bonding role. On the contrary, the same type of antibonding effect between the Mo and $\mu$-Cl atoms is obviously much less prominent in the $14a_1$ orbital of the compound that has a $Mo_3OCl_3$ core. Here the orbital is still predominantly M-M bonding. This is made very clear by comparing the contour plot of the orbital in Figure 3b for $[Mo_3OCl_3(OH)_6(H_2O)_3]^{+}$ with those in parts c and d of Figure 3 for $[Mo_3O_4(OH)_6(H_2O)_3]^{2-}$ and $[Mo_3S_4Cl_6(PH_3)_3]^{2-}$, respectively. These figures may also be compared with the contour plot of the $15a_1$ orbital in Figure 3a for the eight-electron system. It is clear then that the large HOMO-LUMO energy gap and the weakened M-M bonding character in the LUMO are factors that strongly disfavor an eight-electron population for the $M_3O_4$ or $M_4S_4$ core. Conversely, the observed eight- or nine-electron populations in the systems with the $M_3OCl_3$ core is favored by their electronic structures, which are characteristically different from those of the systems with the $M_3O_4$ or $M_3S_4$ core.

The results in Figure 4 also show that for $[Mo_3O_4(OH)_6(H_2O)_3]^{2-}$ the LUMO is not only Mo-($\mu$-O) antibonding and weakly Mo-Mo bonding in character but also almost degenerate with the Mo-Mo antibonding 19e orbital in energy. This may imply that if a compound of similar type but containing seven or eight metal d electrons were to be obtained, the Mo-Mo bond distance would be essentially unchanged or could be even longer than in the case of the six-electron system. This has been found to be true in $Mo_3O_{13}$ in solid state.[19] It may be noted that the Mo-Mo bond distance is shorter in the six-electron system with the $Mo_3O_4$ core (2.49 Å) than in the eight-electron system with the $Mo_3OCl_3$ core (2.58 Å). As we have seen, the M-M bonding effects should be obviously stronger in the eight-electron system, since the two more electrons both go to the MO that is M-M bonding. In addition, the less positive charges on the metal in the eight-electron system should also favor a shorter M-M distance. Therefore, the observed longer Mo-Mo distance in $[Mo_3OCl_6(O_2CCH_3)_3]^{-}$ must be mainly attributed to the larger size of the $\mu$-Cl atom in the $Mo_3OCl_3$ core. The acetate ligand that bridges a pair of Mo atoms in the eight-electron system could be another steric factor favoring the longer Mo-Mo distance. The structural data for a newly characterized trinuclear cluster compound of tungsten[20] show that the distance between the pair of W atoms bridged by two acetate ligands is 0.15 Å longer than that between a pair of W atoms bridged by one acetate ligand and one chlorine atom.

**Acknowledgment.** We thank the National Science Fundation for support.

(19) Torardi, C. C.; McCarley, R. E. *Inorg. Chem.* **1985**, *24*, 476.
(20) Cotton, F. A.; Shang, M.; Sun, Z. To be published.

Contribution from the Department of Chemistry and Laboratory for Molecular Structure and Bonding, Texas A&M University, College Station, Texas 77843

# Synthesis and Characterization of Edge-Sharing Bioctahedral Complexes of Zirconium(III) and Hafnium(III) That Contain Long Metal-Metal Single Bonds: $Zr_2I_6(PMe_3)_4$, $Hf_2I_6(PMe_2Ph)_4$, and $Zr_2I_6(PMe_2Ph)_4$

F. Albert Cotton,* Maoyu Shang, and William A. Wojtczak

*Received March 15, 1991*

The reduction of $MI_4$ (M = Zr, Hf) with 1 equiv of Na/Hg amalgam, followed by addition of 2 equiv of phosphine, produces in moderate yields the edge-sharing bioctahedral complexes $Zr_2I_6(PMe_3)_4$ (**1**), $Hf_2I_6(PMe_2Ph)_4$ (**2**), and $Zr_2I_6(PMe_2Ph)_4$ (**3**). Each compound was characterized by single-crystal X-ray diffraction studies. $Zr_2I_6(PMe_3)_4$ (**1**) crystallizes from *p*-xylene in the monoclinic space group $P2_1/n$ with unit cell dimensions $a$ = 9.752 (2) Å, $b$ = 14.909 (2) Å, $c$ = 11.420 (2) Å, $\beta$ = 96.32 (2)°, $V$ = 1650.3 (6) Å$^3$, and $d_{calc}$ = 2.501 g/cm$^3$ for $Z$ = 2. The structure was refined to $R$ = 0.040 and $R_w$ = 0.050 for 1512 reflections having $I > 3\sigma(I)$. $Hf_2I_6(PMe_2Ph)_4$ (**2**) crystallizes from toluene in the triclinic space group $P\bar{1}$ with unit cell dimensions $a$ = 11.083 (2) Å, $b$ = 11.455 (2) Å, $c$ = 10.081 (2) Å, $\alpha$ = 106.12 (1)°, $\beta$ = 112.17 (1)°, $\gamma$ = 84.70 (1)°, $V$ = 1138.4 (3) Å$^3$, and $d_{calc}$ = 2.438 g/cm$^3$ for $Z$ = 1. The structure was refined to $R$ = 0.037 and $R_w$ = 0.051 for 2855 reflections having $I > 3\sigma(I)$. $Zr_2I_6(PMe_2Ph)_4$ (**3**) is isomorphous to **2** with unit cell dimensions $a$ = 11.132 (2) Å, $b$ = 11.503 (2) Å, $c$ = 10.118 (2) Å, $\alpha$ = 106.17 (1)°, $\beta$ = 112.21 (1)°, $\gamma$ = 84.86 (1)°, $V$ = 1151.9 (3) Å$^3$, and $d_{calc}$ = 2.157 g/cm$^3$ for $Z$ = 1. The structure was refined to $R$ = 0.024 and $R_w$ = 0.039 for 2794 reflections having $I > 3\sigma(I)$. Each of the three complexes has a metal-metal distance of ~3.4 Å. Molecular orbital calculations on the model complex $Zr_2I_6(PH_3)_4$, at the Fenske-Hall level, were conducted to evaluate the bonding between the metal centers. The calculations indicate that the HOMO is metal-metal bonding and mainly composed of metal $d_{z^2}$ and $d_{x^2-y^2}$ $\sigma$-type orbitals.

## Introduction

Although the first examples of edge-sharing bioctahedral complexes of zirconium(III) were reported as early as 1981,[1] it is only within the past few years that further examples of these species,[2] as well as hafnium(III) analogues,[3,4] have been described. These new compounds constitute a significant addition to the

(1) Wengrovius, J. H.; Schrock, R. R.; Day, C. S. *Inorg. Chem.* **1981**, *20*, 1844.
(2) Cotton, F. A.; Diebold, M. P.; Kibala, P. A. *Inorg. Chem.* **1988**, *27*, 799.
(3) Cotton, F. A.; Kibala, P. A.; Wojtczak, W. A. *Inorg. Chim. Acta* **1990**, *177*, 1.

* To whom correspondence should be addressed.

0020-1669/91/1330-3670$02.50/0 

**Table I.** Crystal Data for $Zr_2I_6(PMe_3)_4$ (**1**), $Hf_2I_6(PMe_2Ph)_4$ (**2**), and $Zr_2I_6(PMe_2Ph)_4$ (**3**)

| | **1** | **2** | **3** |
|---|---|---|---|
| formula | $C_{12}H_{36}I_6Zr_2P_4$ | $C_{32}H_{44}I_6Hf_2P_4$ | $C_{32}H_{44}I_6Zr_2P_4$ |
| fw | 1248.2 | 1671.0 | 1496.5 |
| space group | $P2_1/n$ | $P\bar{1}$ | $P\bar{1}$ |
| systematic abs | $(0,k,0)$, $k = 2n + 1$; $(h,0,l)$, $h + l = 2n + 1$ | none | none |
| $a$, Å | 9.752 (2) | 11.083 (2) | 11.132 (2) |
| $b$, Å | 14.909 (2) | 11.455 (2) | 11.503 (2) |
| $c$, Å | 11.420 (2) | 10.081 (2) | 10.118 (2) |
| $\alpha$, deg | 90.00 | 106.12 (1) | 106.17 (1) |
| $\beta$, deg | 96.32 (2) | 112.17 (1) | 112.21 (1) |
| $\gamma$, deg | 90.00 | 84.70 (1) | 84.86 (1) |
| $V$, Å$^3$ | 1650.3 (6) | 1138.4 (3) | 1151.9 (3) |
| $Z$ | 2 | 1 | 1 |
| $d_{calc}$, g/cm$^3$ | 2.501 | 2.438 | 2.157 |
| cryst size, mm | 0.10 × 0.15 × 0.15 | 0.50 × 0.50 × 0.10 | 0.30 × 0.20 × 0.60 |
| $\mu$(Mo K$\alpha$), cm$^{-1}$ | 63.440 | 87.045 | 45.831 |
| data collcn instrument | CAD-4 | Syntex P3/F | Syntex P3/F |
| radiation (monochromated in incident beam) ($\lambda$, Å) | Mo K$\alpha$ (0.710 73) | MoK$\alpha$ (0.710 73) | MoK$\alpha$ (0.710 73) |
| orientation reflcns; no.; range ($2\theta$), deg | 25; 22 < $2\theta$ < 32 | 25; 29 < $2\theta$ < 34 | 25; 33 < $2\theta$ < 34 |
| temp, °C | −50 | 21 | 21 |
| scan method | $\omega$–$2\theta$ | $\omega$–$2\theta$ | $\omega$–$2\theta$ |
| data collcn range ($2\theta$), deg | $4 \le 2\theta \le 46$ | $4 \le 2\theta \le 46$ | $4 \le 2\theta \le 46$ |
| no. of unique data; tot. no. with $F_o^2 > 3\sigma(F_o^2)$ | 2586; 1512 | 2855; 2493 | 3096; 2794 |
| no. of params refined | 109 | 199 | 265 |
| transm factors: max; min | 0.9987; 0.8016 | 0.9937; 0.6653 | 0.9994; 0.8217 |
| $R^a$ | 0.040 33 | 0.037 39 | 0.023 56 |
| $R_w^b$ | 0.049 97 | 0.050 92 | 0.039 40 |
| quality-of-fit indicator[c] | 1.306 | 1.149 | 0.968 |
| largest shift/esd, final cycle | 0.02 | 0.00 | 0.01 |
| largest peak, Å$^3$ | 0.932 | 1.739 | 0.876 |

[a] $R = \sum||F_o| - |F_c||/\sum|F_o|$. [b] $R_w = [\sum w(|F_o| - |F_c|)^2/\sum w|F_o|^2]^{1/2}$; $w = 1/\sigma^2(|F_o|)$. [c] Quality-of-fit = $[\sum w(|F_o| - |F_c|)^2/(N_{observns} - N_{params})]^{1/2}$.

already extensive group of edge-sharing bioctahedral complexes formed by second- and third-row elements in groups V–VIII.[5] In group IV as in other groups, the formation of M–M bonds that generally occur for the metals of the second and third transition series does not occur in corresponding compounds of the metals in the first transition series such as titanium[6] and chromium.[7]

The $Zr_2$ and $Hf_2$ complexes have the longest M–M distances among all the species in which M–M bonds are believed to exist, viz., 3.1–3.2 Å. However, since there are only single bonds and the metal atoms are the largest ones, this need not be considered surprising.

The present work was undertaken in response to the following question. Given that the Zr–Zr and Hf–Hf single-bond distances are already long when the bridging atoms are chlorine atoms, what will be the result of increasing the distances further by employing considerably larger bridging atoms, namely iodine atoms? This could, of course, have made the dimeric structure completely unstable. However, this did not happen, but as anticipated, the M–M distances were considerably increased, to ca. 3.4 Å. At such a distance, is it still reasonable to assign a direct M–M single bond? The answer to this last question will be given in the remainder of this paper.

## Experimental Section

All manipulations were carried out under an argon atmosphere by using standard vacuum-line and Schlenk techniques. The solvents were freshly distilled under nitrogen from the appropriate drying reagent. $HfI_4$, $PMe_3$, and $PMe_2Ph$ were purchased from Strem, and $ZrI_4$ was obtained from Cerac. They were used as received.

**Preparation of $Zr_2I_6(PMe_3)_4$ (1).** $ZrI_4$ (0.599 g, 1.0 mmol) and 1.0 M Na/Hg (1.1 mL, 1.1 mmol) were stirred vigorously in 25 mL of *p*-xylene for 24 h; $PMe_3$ (0.20 mL, 2.0 mmol) was then added dropwise. The reaction was allowed to continue for an additional 12 h. The red-brown solution was then filtered through Celite (2 cm) into a Schlenk tube and layered with 25 mL of hexane. Dark red-brown irregular crystals formed within 1 week. The isolated yield was 250 mg (40%). $^{31}P\{^1H\}$ NMR (81 MHz, $C_7H_8/C_6D_6$, 298 K) referenced to 85% $H_3PO_4$(aq): $\delta$ = −32.00 (s).

**Preparation of $Hf_2I_6(PMe_2Ph)_4$ (2) and $Zr_2I_6(PMe_2Ph)_4$ (3).** Both compounds were synthesized similarly by reduction of $MI_4$ (M = Zr, 0.599 g, 1.0 mmol; M = Hf, 0.686 g, 1.0 mmol) with 1.0 M Na/Hg (1.1 mL, 1.1 mmol) in 20 mL of toluene for 24 h, followed by dropwise addition of $PMe_2Ph$ (0.29 mL, 2.0 mmol). The reactions were allowed to proceed for an additional 24 h following the addition of the $PMe_2Ph$. The resulting brown-green solutions were filtered through Celite (2 cm) into Schlenk tubes and layered with 20 mL of hexane. The Schlenk tubes were placed into a freezer (−20 °C), once the hexane fully diffused into the toluene, and rectangular brown-green crystals appeared within 2 weeks. Isolated yields were 230 mg (28%) for $Hf_2I_6(PMe_2Ph)_4$ and 160 mg (21%) for $Zr_2I_6(PMe_2Ph)_4$.

$^{31}P\{^1H\}$ NMR (81 MHz, $C_7H_8/C_6D_6$, 298 K) referenced to 85% $H_3PO_4$(aq): $\delta$ = −15.23 (s) for $Hf_2I_6(PMe_2Ph)_4$.

## X-ray Crystallography

**Crystal Structure of $Zr_2I_6(PMe_3)_4$ (1).** A small crystal of **1** was mounted on a quartz capillary tip with a thin layer of epoxy cement covering the surface. Geometric and intensity data were taken by an Enraf-Nonius CAD-4 automated diffractometer equipped with graphite-monochromated MO K$\alpha$ ($\lambda$ = 0.710 73 Å) radiation by procedures described previously.[8] All data were collected at −50 °C. The unit cell was indexed on 25 strong reflections in the range $22° \le 2\theta \le 32°$ that were located by an automated search routine. The crystal system was found to be monoclinic. The lattice dimensions were verified by axial oscillation photography. Least-squares analysis was used to refine the cell parameters and orientation matrix.

The intensity data were collected by the $\omega$–$2\theta$ scan technique in the range $4° \le 2\theta \le 46°$. During data collection three intensity standards were collected at 3-h intervals and three orientation reflections were scanned following every 200 reflections. Upon completion of the data collection azimuthal scans of six reflections having the Eulerian angle $\chi$ near 90° were recorded. The data were corrected for Lorentz and polarization factors; decay and semiempirical absorption corrections were also applied.[9a,b]

(4) Girolami, G. S.; Wilson, S. R.; Morse, P. M. *Inorg. Chem.* **1990**, *29*, 3200.
(5) Cotton, F. A. *Polyhedron* **1987**, *6*, 667.
(6) Hermes, A. R.; Girolami, G. S. *Inorg. Chem.* **1990**, *29*, 313.
(7) Cotton, F. A.; Eglin, J. L.; Luck, R. L.; Son, K. A. *Inorg. Chem.* **1990**, *29*, 1802.
(8) (a) Bino, A.; Cotton, F. A.; Fanwick, P. E. *Inorg. Chem.* **1979**, *18*, 3558. (b) Walker, N.; Stuart, D. *Acta Crystallogr., Sect. A.: Found. Crystallogr.* **1983**, *39*, 158.

**Table II.** Positional and Equivalent Isotropic Displacement Parameters and Their Estimated Standard Deviations for $Zr_2I_6(PMe_3)_4$

| atom | x | y | z | $B_{eqv}$,[a] Å$^2$ |
|---|---|---|---|---|
| Zr | 0.5585 (1) | 0.44889 (9) | 0.1283 (1) | 1.93 (3) |
| I(1) | 0.27417 (9) | 0.46255 (7) | 0.02901 (8) | 2.92 (2) |
| I(2) | 0.6134 (1) | 0.27858 (6) | 0.04095 (9) | 3.13 (2) |
| I(3) | 0.5368 (1) | 0.59236 (7) | 0.28357 (9) | 3.28 (2) |
| P(1) | 0.8183 (4) | 0.4375 (3) | 0.2558 (4) | 2.87 (8) |
| P(2) | 0.4260 (4) | 0.3459 (3) | 0.2845 (3) | 2.81 (8) |
| C(1) | 0.940 (2) | 0.361 (1) | 0.194 (2) | 5.0 (4) |
| C(2) | 0.918 (2) | 0.541 (1) | 0.267 (2) | 4.8 (4) |
| C(3) | 0.832 (2) | 0.402 (2) | 0.410 (1) | 5.8 (5) |
| C(4) | 0.314 (2) | 0.408 (1) | 0.368 (1) | 3.8 (4) |
| C(5) | 0.525 (2) | 0.281 (1) | 0.402 (1) | 4.5 (4) |
| C(6) | 0.312 (2) | 0.259 (1) | 0.215 (2) | 3.9 (4) |

[a] *B* values for anisotropically refined atoms are given in the form of the equivalent isotropic displacement parameter defined as $(4/3)[a^2\beta_{11} + b^2\beta_{22} + c^2\beta_{33} + ab(\cos\gamma)\beta_{12} + ac(\cos\beta)\beta_{13} + bc(\cos\alpha)\beta_{23}]$.

**Table III.** Positional and Equivalent Isotropic Displacement Parameters and Their Estimated Standard Deviations for $Hf_2I_6(PMe_2Ph)_4$

| atom | x | y | z | $B_{eqv}$[a] Å$^2$ |
|---|---|---|---|---|
| Hf | 0.59340 (4) | 0.38595 (4) | 0.44377 (4) | 2.61 (1) |
| I(1) | 0.55638 (7) | 0.44856 (7) | 0.72003 (7) | 3.31 (2) |
| I(2) | 0.82437 (7) | 0.51678 (7) | 0.56531 (9) | 3.81 (2) |
| I(3) | 0.40597 (7) | 0.19915 (7) | 0.29701 (9) | 4.17 (2) |
| P(1) | 0.7343 (3) | 0.2005 (3) | 0.5627 (3) | 3.16 (7) |
| P(2) | 0.6557 (3) | 0.3182 (3) | 0.1920 (3) | 3.16 (7) |
| C(11) | 0.652 (1) | 0.130 (1) | 0.651 (1) | 4.9 (3) |
| C(12) | 0.768 (2) | 0.062 (1) | 0.438 (1) | 5.3 (4) |
| C(13) | 0.891 (1) | 0.245 (1) | 0.711 (1) | 3.5 (3) |
| C(14) | 0.900 (2) | 0.295 (1) | 0.854 (1) | 5.4 (4) |
| C(15) | 1.028 (2) | 0.334 (1) | 0.966 (2) | 7.1 (5) |
| C(16) | 1.134 (2) | 0.320 (1) | 0.926 (2) | 7.5 (5) |
| C(17) | 1.126 (1) | 0.272 (1) | 0.783 (2) | 6.7 (4) |
| C(18) | 1.005 (1) | 0.236 (1) | 0.677 (2) | 5.8 (4) |
| C(21) | 0.718 (1) | 0.444 (1) | 0.155 (1) | 5.0 (3) |
| C(22) | 0.518 (1) | 0.261 (1) | 0.017 (1) | 5.5 (4) |
| C(23) | 0.779 (1) | 0.205 (1) | 0.177 (1) | 3.1 (2) |
| C(24) | 0.751 (1) | 0.085 (1) | 0.083 (1) | 4.8 (3) |
| C(25) | 0.848 (2) | 0.003 (1) | 0.080 (2) | 6.3 (4) |
| C(26) | 0.979 (1) | 0.034 (1) | 0.170 (2) | 5.5 (4) |
| C(27) | 1.007 (1) | 0.152 (1) | 0.259 (1) | 5.4 (4) |
| C(28) | 0.908 (1) | 0.237 (1) | 0.265 (1) | 4.4 (3) |

[a] *B* values for anisotropically refined atoms are given in the form of the equivalent isotropic displacement parameter defined as $(4/3)[a^2\beta_{11} + b^2\beta_{22} + c^2\beta_{33} + ab(\cos\gamma)\beta_{12} + ac(\cos\beta)\beta_{13} + bc(\cos\alpha)\beta_{23}]$.

The structure was refined successfully in the uniquely defined monoclinic space group $P2_1/n$. The initial positions of the crystallographically unique zirconium and iodine atoms were obtained by direct methods.[9c] Development of the rest of the structure then proceeded routinely. The non-hydrogen atoms were located with alternating sequences of least-squares refinement and difference Fourier maps. All atoms were refined anisotropically. The final Fourier map showed only randomly distributed low electron density peaks. Table I summarizes the data pertaining to the crystallographic procedures and refinement of complexes **1**–**3**. The atomic positional parameters of **1** are listed in Table II.

**Crystal Structure of $Hf_2I_6(PMe_2Ph)_4$ (2).** The general procedures were routine and similar to those just described. A small rectangular crystal of **2** was affixed to the inside of a thin-walled capillary with epoxy cement. The capillary was then mounted on the goniometer head of a P3/F diffractometer. The data were collected as indicated in Table I. Lorentz, polarization, decay, and semiempirical absorption corrections were applied to the data.[9d] The solution and refinement of the structure proceeded smoothly in the triclinic space group $P\bar{1}$. The initial positions of the hafnium and iodine atoms were ascertained from direct methods.[9c] The positions of all other non-hydrogen atoms were obtained from iterative applications of least-squares refinement and difference Fourier maps. The atomic positional parameters are given in Table III.

**Table IV.** Positional and Equivalent Isotropic Displacement Parameters and Their Estimated Standard Deviations for $Zr_2I_6(PMe_2Ph)_4$

| atom | x | y | z | $B_{eqv}$,[a] Å$^2$ |
|---|---|---|---|---|
| Zr | 0.59417 (4) | 0.38517 (4) | 0.44337 (4) | 2.37 (1) |
| I(1) | 0.55660 (3) | 0.44841 (3) | 0.72039 (3) | 3.258 (8) |
| I(2) | 0.82663 (3) | 0.51588 (3) | 0.56512 (4) | 3.749 (9) |
| I(3) | 0.40740 (4) | 0.19613 (3) | 0.29553 (4) | 4.140 (9) |
| P(1) | 0.7363 (1) | 0.1989 (1) | 0.5639 (1) | 3.02 (3) |
| P(2) | 0.6560 (1) | 0.3167 (1) | 0.1887 (1) | 3.11 (3) |
| C(11) | 0.6561 (6) | 0.1279 (5) | 0.6496 (6) | 4.8 (1) |
| C(12) | 0.7719 (7) | 0.0630 (5) | 0.4382 (7) | 4.8 (2) |
| C(13) | 0.8932 (5) | 0.2443 (5) | 0.7113 (6) | 3.5 (1) |
| C(14) | 0.9036 (7) | 0.2932 (7) | 0.8549 (7) | 5.7 (2) |
| C(15) | 1.0226 (8) | 0.3334 (7) | 0.9661 (9) | 7.6 (2) |
| C(16) | 1.1344 (7) | 0.3223 (7) | 0.9312 (9) | 7.2 (2) |
| C(17) | 1.1248 (7) | 0.2753 (7) | 0.7917 (9) | 7.1 (2) |
| C(18) | 1.0074 (6) | 0.2340 (6) | 0.6808 (7) | 5.5 (2) |
| C(21) | 0.7183 (6) | 0.4403 (5) | 0.1517 (6) | 4.6 (1) |
| C(22) | 0.5168 (6) | 0.2630 (7) | 0.0145 (6) | 5.0 (2) |
| C(23) | 0.7799 (5) | 0.2023 (5) | 0.1767 (5) | 3.2 (1) |
| C(24) | 0.7497 (6) | 0.0859 (5) | 0.838 (6) | 4.4 (2) |
| C(25) | 0.8486 (7) | 0.0041 (6) | 0.0820 (7) | 6.0 (2) |
| C(26) | 0.9770 (7) | 0.0363 (6) | 0.1702 (7) | 5.7 (2) |
| C(27) | 1.0070 (6) | 0.1511 (6) | 0.2597 (8) | 5.4 (2) |
| C(28) | 0.9070 (5) | 0.2353 (5) | 0.2621 (6) | 4.0 (1) |
| H(111) | 0.708 (7) | 0.060 (7) | 0.687 (9) | 6.2* |
| H(112) | 0.589 (7) | 0.102 (7) | 0.590 (8) | 6.2* |
| H(113) | 0.661 (8) | 0.183 (7) | 0.724 (8) | 6.2* |
| H(121) | 0.824 (7) | 0.006 (7) | 0.522 (8) | 6.2* |
| H(122) | 0.688 (7) | 0.022 (7) | 0.369 (8) | 6.2* |
| H(123) | 0.835 (7) | 0.090 (7) | 0.420 (8) | 6.2* |
| H(14) | 0.834 (8) | 0.281 (8) | 0.881 (9) | 7.3* |
| H(15) | 1.030 (9) | 0.387 (9) | 1.06 (1) | 9.8* |
| H(16) | 1.227 (9) | 0.338 (8) | 1.04 (1) | 9.4* |
| H(17) | 1.195 (9) | 0.248 (9) | 0.77 (1) | 9.4* |
| H(18) | 1.005 (8) | 0.219 (7) | 0.588 (9) | 7.0* |
| H(211) | 0.747 (7) | 0.393 (7) | 0.063 (8) | 6.0* |
| H(212) | 0.632 (8) | 0.496 (7) | 0.117 (8) | 6.0* |
| H(213) | 0.782 (7) | 0.456 (7) | 0.209 (8) | 6.0* |
| H(221) | 0.508 (7) | 0.186 (7) | 0.024 (8) | 6.2* |
| H(222) | 0.550 (7) | 0.241 (7) | −0.048 (8) | 6.2* |
| H(223) | 0.462 (7) | 0.339 (7) | 0.016 (8) | 6.2* |
| H(24) | 0.686 (7) | 0.069 (7) | 0.032 (8) | 6.0* |
| H(25) | 0.857 (8) | −0.103 (8) | 0.029 (1) | 7.8* |
| H(26) | 1.040 (8) | −0.014 (8) | 0.16 (1) | 7.8* |
| H(27) | 1.107 (8) | 0.183 (8) | 0.339 (9) | 7.0* |
| H(28) | 0.911 (7) | 0.317 (6) | 0.309 (8) | 5.1* |

[a] Starred *B* values correspond to atoms that had their thermal parameter fixed and were refined isotropically. *B* values for anisotropically refined atoms are given in the form of the equivalent isotropic displacement parameter defined as $(4/3)[a^2\beta_{11} + b^2\beta_{22} + c^2\beta_{33} + ab(\cos\gamma)\beta_{12} + ac(\cos\beta)\beta_{13} + bc(\cos\alpha)\beta_{23}]$.

**Crystal Structure of $Zr_2I_6(PMe_2Ph)_4$ (3).** A crystalline plate of **3** was glued to the inside of a thin-walled capillary with epoxy cement. The data were collected on a P3/F diffractometer by using procedures previously outlined. Lorentz, polarization, decay, and semiempirical absorption corrections were applied to the data.[9d] The structure was refined in the triclinic space group $P\bar{1}$. Preliminary coordinates of **3** were taken from the isomorphous hafnium complex, **2**. All non-hydrogen atoms were refined anisotropically. Hydrogen atoms of **3** were found from a difference Fourier map that followed the anisotropic refinement of all the non-hydrogen atoms. The thermal parameters of the hydrogen atoms were fixed at 1.3 times the equivalent isotropic thermal parameter of the carbon atoms to which they are bound. The atomic positional parameters are listed in Table IV.

## Computational Procedures

Molecular orbital calculations[10] on the model compound $Zr_2I_6(PH_3)_4$ were carried out by applying the Fenske–Hall approximation to the

(9) (a) North, A. C. T.; Phillips, D. C.; Mathews, F. S. *Acta Crystallogr., Sect. A: Cryst. Phys. Diffr., Theor. Gen. Crystallogr.* **1968**, *A24*, 351. (b) The calculations were performed with the Enraf-Nonius Structure Determination Package on the VAX 11/780 computer at the Department of Chemistry, Texas A&M University, College Station, TX 77843. (c) Sheldrick, G. M. *SHELX-86, Program for Crystal Structure Determination*; University of Cambridge: Cambridge, England, 1986. (d) Sheldrick, G. M. *SHELX-76, Program for Crystal Structure Determination*; University of Cambridge: Cambridge, England, 1976.

(10) The calculations were performed on the Microvax II computer at the Laboratory for Molecular Structure and Bonding, Texas A&M University.

Hartree–Fock molecular orbital method.[11] Metal atom basis functions were taken from Richardson[12] and were extended to include 5s and 5p zirconium functions with an exponent of 2.20.[13] Clementi $\zeta$ basis sets[14] were used for the main-group elements, phosphorus, iodine, and hydrogen. The hydrogen atom exponent was set at 1.20. The atomic coordinates used in the calculation were taken from the crystal structure data of **1** and idealized to conform with the $D_{2h}$ symmetry of the model. The hydrogen atom coordinates were calculated to preserve the $D_{2h}$ symmetry. The coordinate system for $Zr_2I_6(PH_3)_4$ was chosen so that the origin was placed at the midpoint of the Zr–Zr vector. The molecular $z$ axis is located along the Zr–Zr vector, and the $x$ axis lies in the $Zr_2(I_b)_2$ plane. For each atom a local right-handed coordinate system was designated as follows: the $z$ axis of the local system points toward the origin for the zirconium atoms and toward the zirconium atoms for the iodine and phosphorus atoms. The $z$ axis of the hydrogen atoms pointed toward the phosphorus to which they were bound.

## Results and Discussion

The literature is replete with examples of edge-sharing bioctahedral complexes of general formulas $M_2X_6L_4$ and $M_2X_6(LL)_2$,[15] but only one fully characterized example has been made for X = I, namely, $Mo_2I_6(dppm)_2$.[16] We have synthesized and fully characterized by X-ray crystallography and $^{31}P\{^1H\}$ NMR spectroscopy the iodide-bridged analogues of previously reported edge-sharing bioctahedral complexes of zirconium(III) and hafnium(III). Our structural, spectroscopic ($^{31}P\{^1H\}$ NMR), and theoretical data suggest that these iodide-bridged complexes can be formulated, as have been their chloride-bridged predecessors, as diamagnetic dimers with substantial amounts of metal–metal bonding. The phosphine ligands in all examples of these complexes, to date, lie within the $M_2(X_b)_2$ plane.[2-4,6] This creates the distinctive cis–cis geometry with respect to the two metal centers (I). Edge-sharing bioctahedral complexes with monodentate ligands from groups V and VI, namely, $Ta_2Cl_6(PMe_3)_4$[17] and

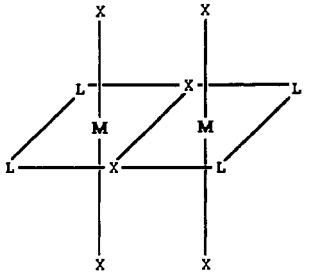


I

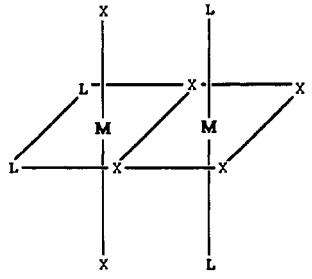


II

$W_2Cl_6(Py)_4$,[18] exhibit the cis–trans arrangement (II). The particular combinations of electronic and steric factors that favor one structure type over the other have not yet been identified.

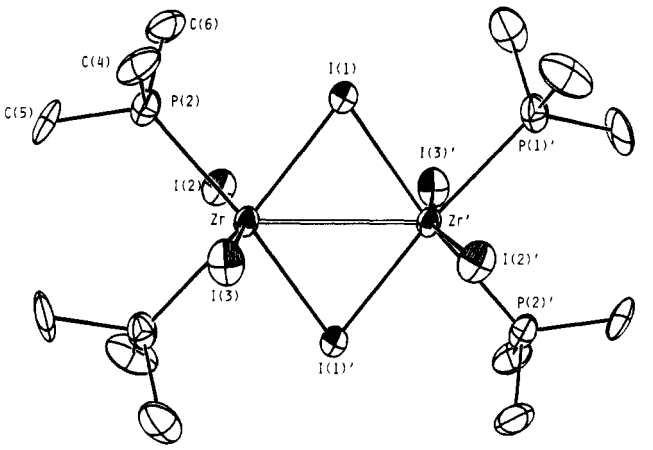


**Figure 1.** Top view of $Zr_2I_6(PMe_3)_4$ (**1**). Atoms are represented by their ellipsoids at the 50% probability level.

**Table V.** Selected Listing of Bond Distances (Å) and Angles (deg) for $Zr_2I_6(PMe_3)_4$[a]

| | | | |
|---|---|---|---|
| Zr–Zr' | 3.393 (2) | P(1)–C(1) | 1.84 (2) |
| Zr–I(1) | 2.890 (2) | P(1)–C(2) | 1.82 (2) |
| Zr–I(1)' | 2.881 (2) | P(1)–C(3) | 1.84 (2) |
| Zr–I(2) | 2.805 (2) | P(2)–C(4) | 1.79 (2) |
| Zr–I(3) | 2.805 (2) | P(2)–C(5) | 1.84 (2) |
| Zr–P(1) | 2.788 (4) | P(2)–C(6) | 1.84 (2) |
| Zr–P(2) | 2.782 (4) | | |
| Zr–Zr'–I(1) | 53.86 (4) | Zr–P(1)–C(2) | 115.7 (6) |
| Zr–Zr'–I(1) | 54.10 (4) | Zr–P(1)–C(3) | 119.2 (6) |
| Zr–Zr'–I(2) | 99.14 (5) | C(1)–P(1)–C(2) | 101.2 (8) |
| Zr–Zr'–I(3) | 99.35 (5) | C(1)–P(1)–C(3) | 101.9 (9) |
| Zr–Zr'–P(1) | 132.9 (1) | C(2)–P(1)–C(3) | 101.1 (9) |
| Zr–Zr'–P(2) | 131.88 (9) | Zr–P(2)–C(4) | 114.1 (6) |
| I(1)–Zr–I(1)' | 107.96 (5) | Zr–P(2)–C(5) | 121.0 (6) |
| I(2)–Zr–I(3) | 161.50 (6) | Zr–P(2)–C(6) | 114.7 (6) |
| P(1)–Zr–P(2) | 95.2 (1) | C(4)–P(2)–C(5) | 101.0 (8) |
| Zr–I(1)–Zr | 72.04 (4) | C(4)–P(2)–C(6) | 102.8 (8) |
| Zr–P(1)–C(1) | 115.1 (6) | C(5)–P(2)–C(6) | 100.6 (8) |

[a] Numbers in parentheses are estimated standard deviations in the least significant digits.

An ORTEP drawing of compound **1**, showing a top view, is presented in Figure 1. The only rigorous symmetry of **1** is $\bar{1}$, but it possesses, effectively, the higher symmetry $D_{2h}$, where the three mutually perpendicular $C_2$ axes bisect the Zr–Zr vector. A selected listing of bond distances and angles for **1** is presented in Table V. The average Zr–$I_b$ distance (2.886 [6] Å) of **1** is significantly longer, by 0.081 (6) Å, than the Zr–$I_t$ (2.805 (2) Å) distance, as expected. The degree of metal–metal interaction has in the past been correlated to the M–M distance and the angular parameters $X_t$–M–$X_t$, $X_b$–M–$X_b$, and M–$X_b$–M.[2-4,6] A strong repulsion between the adjacent pairs of terminal iodine atoms is evident from both Figure 1 and the I(2)–Zr–I(3) angle, which is 18.5° below 180°. The I(1)–Zr–I(1)' and Zr–I(1)–Zr' angles suggest that there is a direct attraction between zirconium centers. In fact, the aforementioned angles deviate, by a larger degree, from ideal bioctahedral geometry, than those reported for the chloride-bridged dimers. A comparison of these and other structural parameters, for all reported group IV metal edge-sharing dimers, is given in Table VI. Thus, the structure parameters in the $\mu$-I compounds afford a prima facia case for the existence of direct M–M bonds. However, to bolster this, the question of whether zirconium or hafnium atoms at distances of ~3.4 Å can

(11) Fenske, R. F.; Hall, M. B. *Inorg. Chem.* **1972**, *11*, 768.
(12) Richardson, J. W.; Blackman, M. J.; Ranochak, J. E. *J. Chem. Phys.* **1973**, *58*, 3010.
(13) Barber, M.; Connor, J. A.; Guest, M. F.; Hall, M. B.; Hiller, I. H.; Meredith, W. N. E. *J. Chem. Soc., Faraday Trans. 2* **1972**, *54*, 219.
(14) *Table of Atomic Functions*. A supplement of a paper by: Clementi, E. *IBM J. Res. Dev.* **1965**, *9*, 2.
(15) For a general overview, see: (a) Cotton, F. A. Metal Metal Bonds in Edge Sharing Bioctahedra. In *Understanding Molecular Properties*, Avery, J., et al., Eds.; D. Riedel Publishing Co.: Dordrecht, The Netherlands, 1987; pp 17–26. See also ref 5.
(16) Cotton, F. A.; Daniels, L. M.; Dunbar, K. R.; Falvello, L. R.; O'Connor, C. J.; Price, A. C. *Inorg. Chem.* **1991**, *30*, 2552.
(17) Sattelberger, A. P.; Wilson, R. B., Jr.; Huffman, C. J. *Inorg. Chem.* **1982**, *21*, 2392.
(18) Jackson, R. B.; Streib, W. E. *Inorg. Chem.* **1971**, *10*, 1760.

**Table VI.** Selected Bond Distances (Å) and Angles (deg) for $M_2X_6(L)_4$ and $M_2X_6(LL)_2$ (M = Ti, Zr, Hf) Type Compounds

| | M-M | M-P | P-M-P | $X_b$-M-$X_b$ | $X_t$-M-$X_t$ | M-$X_b$-M | source |
|---|---|---|---|---|---|---|---|
| $Zr_2I_6(PMe_3)_4$ | 3.393 (2)[b] | 2.785 [3][c] | 95.2 (1) | 107.96 (5) | 161.50 (6) | 72.04 (4) | this work |
| $Hf_2I_6(PMe_2Ph)_4$ | 3.3948 (6) | 2.777 [11] | 94.60 (9) | 107.03 (3) | 163.30 (3) | 72.97 (2) | this work |
| $Zr_2I_6(PMe_2Ph)_4$ | 3.4390 (6) | 2.812 [11] | 94.75 (4) | 106.64 (2) | 162.58 (2) | 73.36 (2) | this work |
| $Ti_2Cl_6(dippe)_2$ | 3.438 (2) | 2.652 [7] | 78.6 (2) | 91.4 (1) | 169.6 (2) | 88.6 (1) | ref 6 |
| $Hf_2Cl_6(dippe)_2$ | 3.102 (3) | 2.746 [3] | 76.7 (1) | 104.0 (1) | 166.5 (1) | 76.0 (1) | ref 4 |
| $Zr_2Cl_6(dppe)_2$[a] | 3.099 (2) | 2.778 [7] | 76.25 (9) | 104.52 (8) | 161.8 (1) | 75.48 (8) | ref 2 |
| | 3.109 (2) | 2.785 [23] | 75.64 (9) | 104.62 (8) | 163.8 (1) | 75.38 (8) | |
| $Zr_2Cl_6(PMe_2Ph)_4$ | 3.127 (1) | 2.765 [5] | 96.19 (8) | 104.26 (8) | 162.1 (1) | 75.74 (7) | ref 2 |
| $Hf_2Cl_6(PMe_2Ph)_4$ | 3.0886 (3) | 2.752 [14] | 96.02 (5) | 104.55 (5) | 162.89 (5) | 75.45 (4) | ref 3 |
| $Zr_2Cl_6(PEt_3)_4$ | 3.169 (1) | 2.813 [7] | 96.02 (6) | 102.81 (5) | 163.77 (6) | 77.19 (4) | ref 2 |
| $Zr_2Cl_6(PBu_3)_4$ | 3.182 (1) | 2.834 [4] | 96.25 (5) | 102.57 (5) | 165.11 (6) | 77.43 (4) | ref 1 |

[a] There are two independent dimers in the unit cell. [b] Parentheses denote esd of an individual value. [c] Square brackets denote mean deviation from the unweighted arithmetic mean; each is given for the last significant figure.

**Table VII.** Selected Listing of Bond Distances (Å) and Angle (deg) for $Hf_2I_6(PMe_2Ph)_4$[a]

| | | | |
|---|---|---|---|
| Hf-Hf′ | 3.3948 (6) | Hf-I(3) | 2.7976 (8) |
| Hf-I(1) | 2.8526 (9) | Hf-P(1) | 2.788 (3) |
| Hf-I(1)′ | 2.8571 (9) | Hf-P(2) | 2.766 (3) |
| Hf-I(2) | 2.7607 (8) | | |
| I(1)-Hf-I(1)′ | 107.03 (3) | I(1)′-Hf-P(2) | 78.07 (6) |
| I(1)-Hf-I(2) | 92.57 (3) | I(2)-Hf-I(3) | 163.30 (3) |
| I(1)-Hf-I(3) | 96.88 (3) | I(2)-Hf-P(1) | 87.47 (6) |
| I(1)-Hf-P(1) | 80.54 (7) | I(2)-Hf-P(2) | 83.55 (6) |
| I(1)-Hf-P(2) | 173.94 (6) | I(3)-Hf-P(1) | 80.57 (6) |
| I(1)′-Hf-I(2) | 95.88 (3) | I(3)-Hf-P(2) | 85.82 (6) |
| I(1)′-Hf-I(3) | 94.48 (2) | P(1)-Hf-P(2) | 94.60 (9) |
| I(1)′-Hf-P(1) | 171.51 (6) | Hf-I(1)-Hf′ | 72.97 (2) |

[a] Numbers in parentheses are estimated standard deviations in the least significant digits.

**Table VIII.** Selected Listing of Bond Distances (Å) and Angles (deg) for $Zr_2I_6(PMe_2Ph)_4$[a]

| | | | |
|---|---|---|---|
| Zr-Zr′ | 3.4390 (6) | Zr-I(3) | 2.8173 (5) |
| Zr-I(1) | 2.8735 (6) | Zr-P(1) | 2.823 (1) |
| Zr-I(1)′ | 2.8834 (6) | Zr-P(2) | 2.801 (2) |
| Zr-I(2) | 2.7804 (6) | | |
| I(1)-Zr-I(1)′ | 106.64 (2) | I(1)′-Zr-P(2) | 78.23 (3) |
| I(1)-Zr-I(2) | 92.82 (1) | I(2)-Zr-I(3) | 162.58 (2) |
| I(1)-Zr-I(3) | 97.04 (2) | I(2)-Zr-P(1) | 87.18 (3) |
| I(1)-Zr-P(1) | 80.61 (3) | I(2)-Zr-P(2) | 83.50 (3) |
| I(1)-Zr-P(2) | 174.25 (3) | I(3)-Zr-P(1) | 80.34 (3) |
| I(1)′-Zr-I(2) | 96.07 (2) | I(3)-Zr-P(2) | 85.46 (3) |
| I(1)′-Zr-I(3) | 94.81 (1) | P(1)-Zr-P(2) | 94.75 (4) |
| I(1)′-Zr-P(1) | 171.83 (3) | Zr-I(1)-Zr′ | 73.36 (2) |

[a] Numbers in parentheses are estimated standard deviations in the least significant digits.

be accurately described as being bound by a direct through-space metal-metal orbital interaction will be discussed within the context of our theoretical calculations.

An ORTEP drawing of compound **2**, showing a side view, is depicted in Figure 2. Selected listings of bond distances and angles for compounds **2** and **3** are given in Tables VII and VIII, respectively. Compounds **2** and **3** are isomorphous and have molecular dimensions that closely parallel one another, arising from the similarity in radial size of zirconium and hafnium atoms that are within the same chemical and structural environment. The Hf-Hf distance in **2** (3.3948 (6) Å) is significantly shorter, by .044 Å, than the Zr-Zr distance (3.4390 (6) Å) in **3**. This is not surprising, since it has been observed that, within the same structural context, third-row transition metals give shorter M-M distances than their second row counterparts.

A comparison of $Zr_2I_6(PMe_2Ph)_4$ and $Hf_2I_6(PMe_2Ph)_4$ with $Zr_2Cl_6(PMe_2Ph)_4$ and $Hf_2Cl_6(PMe_2Ph)_4$ (see Table VI) shows, as expected, that the M-M distance lengthens considerably in the iodide-bridged compounds. The angular parameters, $X_b$-M-$X_b$ and M-$X_b$-M, surprisingly, are significantly more obtuse and acute, respectively, for X = I than for X = Cl. This is another indication that the attractive force between the metal centers

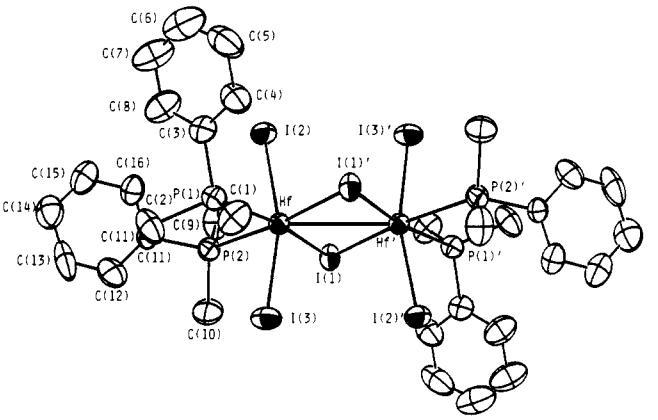


**Figure 2.** Side view of $Hf_2I_6(PMe_2Ph)_4$ (**2**). Atoms are represented by their ellipsoids at the 50% probability level.

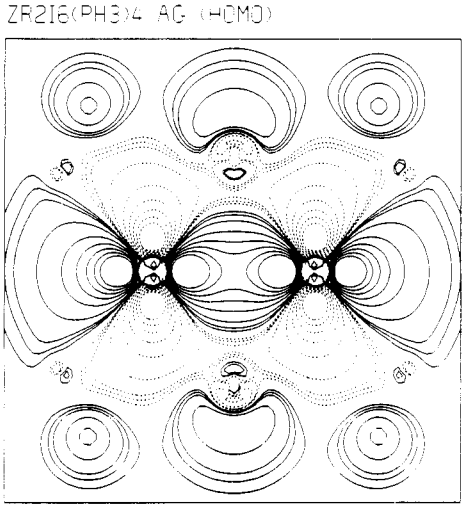


**Figure 3.** Contour plot of the $A_g$ HOMO of $Zr_2I_6(PH_3)_4$, in the *xz* plane.

remains substantial, even for the long M-M distances imposed by the iodide bridging atoms. In fact, there is some indication that zirconium complexes with M-M distances of 3.5-3.7 Å retain considerable amounts of metal-metal interaction.[19-22]

Having established some structural features of the $M_2X_6L_4$ complexes (M = Ti, Zr, Hf; X = Cl, I; L = $PR_3$), we can now turn our attention to the description of their bonding from a theoretical viewpoint. We conducted a Fenske-Hall molecular orbital treatment on the model compound $Zr_2I_6(PH_3)_4$.[11] The

(19) Chiang, M. Y.; Gambarotta, S.; van Bolhius, S. *Organometallics* **1988**, *7*, 1864.
(20) Wielstra, Y.; Gambarotta, S.; Meetsma, A.; de Boer, J. L. *Organometallics* **1989**, *8*, 250.
(21) Wielstra, Y.; Gambarotta, S.; Meetsma, A.; Spek, A. L. *Organometallics* **1989**, *8*, 2948.
(22) Rohmer, M. M.; Benard, M. *Organometallics* **1991**, *10*, 157.

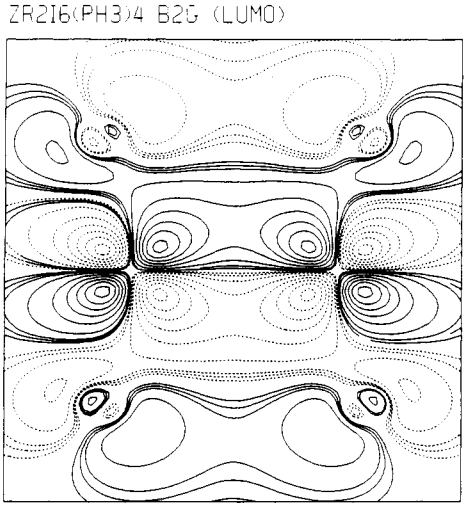


**Figure 4.** Contour plot of the $B_{2g}$ LUMO of $Zr_2I_6(PH_3)_4$, in the *xz* plane.

calculation resulted in a molecular orbital diagram with 41 doubly occupied valence orbitals. The HOMO is formed, primarily, from a combination of zirconium $d_{z^2}$ and $d_{x^2-y^2}$ orbitals (the combined metal character is 92.6%). The bridging iodide atoms interact only weakly along the Zr-$I_b$ vectors, through a linear combination of their $p_y$ and $p_z$ orbitals (combined $I_b$ character in the HOMO is 2.8%). We and others believe that the long metal-metal interaction in these complexes is best described as being, primarily, through-space.[22] A contour plot of the HOMO of $Zr_2I_6(PH_3)_4$, in the *xz* plane, is given in Figure 3. Clearly, this orbital provides a significant M-M $\sigma$ bond. The LUMO is composed of zirconium $d_{xz}$ $\pi$-type orbitals, which lie in a plane perpendicular to the $Zr_2(I_b)_2$ plane. A contour plot of the LUMO, in the *xz* plane, is given in Figure 4.

### Concluding Remarks

The $M_2I_6(PR_3)_4$ complexes are structurally similar to previously reported group IV metal chloride-bridged bioctahedral complexes, the main distinction being the considerably longer metal-metal distance. Structural and theoretical data concur in suggesting that these diamagnetic complexes are correctly formulated with long but real metal-metal single bonds. We are currently attempting to synthesize and structurally characterize edge-sharing dimers of zirconium and hafnium with other atoms in the bridging position, for comparative purposes.

**Acknowledgment.** We thank Judith L. Eglin for carrying out the $^{31}P$ NMR spectroscopy and the Robert A. Welch Foundation for support under Grant A 494.

**Supplementary Material Available:** Full listings of bond lengths and angles, thermal displacements, and valence molecular orbitals, their energies, and percent characters for $Zr_2I_6(PH_3)_6$ (39 pages); tables of observed and calculated structure factors for **1-3** (35 pages). Ordering information is given on any current masthead page.

---

Contribution from the Department of Chemistry and Laboratory for Molecular Structure and Bonding, Texas A&M University, College Station, Texas 77843

# Preparation and Molecular and Electronic Structures of a New Diamagnetic Diruthenium(II) Complex, $Ru_2[(p\text{-tol})NC(H)N(p\text{-tol})]_4$

F. Albert Cotton* and Tong Ren

*Received March 15, 1991*

The title complex, $Ru_2(DFM)_4$ ($DFM^-$ = (*p*-tol)NCHN(*p*-tol)$^-$), has been synthesized and characterized by X-ray crystallography as well as several spectroscopic methods. The dark red complex crystallizes as $Ru_2(DFM)_4 \cdot C_6H_6$ in space group *Pbnb* with $a$ = 17.086 (4) Å, $b$ = 23.952 (11) Å, $c$ = 15.521 (4) Å, $V$ = 6352 (4) Å$^3$, and $Z$ = 4. The complex has been shown to be diamagnetic on the basis of $^1H$ NMR spectroscopy and has a very long Ru-Ru distance (2.474 (1) Å). These features are indicative of a $(\sigma)^2(\pi)^4(\delta)^2(\pi^*)^4$ ground-state configuration. A fairly large $\delta^*-\pi^*$ gap (1.18 eV) was derived from an SCF-X$\alpha$ calculation performed on the model $Ru_2(HNCHNH)_4$, thus confirming the configuration mentioned above. The observed electronic absorption spectrum was assigned with the aid of the MO calculation.

### Introduction

Recent studies of diruthenium chemistry have shown that the diruthenium(II) complexes, that is, those with a $Ru_2^{4+}$ core, provide a valuable test ground for the development of metal-metal bonding theory.[1-9] As discussed earlier for various $Ru_2(LL)_4$ species,[2,5,8] for a $d^6$-$d^6$ system in an effective $D_{4h}$ symmetry there are three possible ground-state configurations beyond the $(\sigma)^2(\pi)^4(\delta)^2$ shells, namely, $(\pi^*)^4$, $(\pi^*)^3(\delta^*)$, and $(\pi^*)^2(\delta^*)^2$. The category to which a particular complex belongs is determined by the $\delta^*-\pi^*$ separation, which is in turn determined by the $\pi$ basicity of the bridging ligand $LL^-$. Among all known diruthenium(II) complexes, triazeno complexes distinguish themselves in being diamagnetic at room temperature and having a very long Ru-Ru bond length.[4-6] A large $\delta^*-\pi^*$ gap of 0.98 eV was found through a model X$\alpha$ calculation,[7] which, in conjunction with the structural and NMR evidence, has convincingly shown that $(\pi^*)^4$ is the ground-state configuration. Here we report the synthesis and various characterizations of another diamagnetic diruthenium(II) complex, $Ru_2[(p\text{-tol})NCHN(p\text{-tolyl})]_4$.

### Experimental Section

The synthesis and the spectroscopic characterizations were carried out in argon atmosphere by using standard Schlenkware and some other air-tight containers. $Ru_2(OAc)_4$ was prepared by refluxing the reduced "blue solution" of ruthenium trichloride with LiOAc in MeOH under argon;[1] di-*p*-tolylformamidine (HDFM) was obtained by the direct condensation between triethyl orthoformate and *p*-toluidine.[10] All the solvents used were freshly distilled over suitable drying reagents under $N_2$.

**Preparation of $Ru_2(DFM)_4$.** A 1.01-g amount of HDFM (4.5 mmol) was dissolved in 15 mL of THF, and the solution was then neutralized

* To whom correspondence should be addressed.

(1) Lindsay, A. J.; Wilkinson, G.; Motevalli, M.; Hursthouse, M. B. *J. Chem. Soc., Dalton Trans.* **1985**, 2321.
(2) Cotton, F. A.; Miskowski, V. M.; Zhong, B. *J. Am. Chem. Soc.* **1989**, *111*, 6177.
(3) Maldivi, P.; Giroud-Godquin, A.; Marchon, J.; Guillon, D.; Skoulios, A. *Chem. Phys. Lett.* **1989**, *157*, 552.
(4) Lindsay, A. J.; Wilkinson, G.; Motevalli, M.; Hursthouse, M. B. *J. Chem. Soc., Dalton Trans.* **1987**, 2723.
(5) Cotton, F. A.; Matusz, M. *J. Am. Chem. Soc.* **1988**, *110*, 5761.
(6) Cotton, F. A.; Falvello, L. R.; Ren, T.; Vidyasagar, K. Manuscript in preparation.
(7) Cotton, F. A.; Feng, X. *Inorg. Chem.* **1989**, *28*, 1180.
(8) Cotton, F. A.; Ren, T.; Eglin, J. L. *J. Am. Chem. Soc.* **1990**, *112*, 3439.
(9) Cotton, F. A.; Ren, T.; Eglin, J. L. *Inorg. Chem.* **1991**, *30*, 2552.
(10) Bradley, W.; Wright, I. *J. Chem. Soc.* **1956**, 640.

0020-1669/91/1330-3675$02.50/0 